International Journal of Applied Engineering Research ISSN 0973-4562 Volume 16, Number 3 (2021) pp. 192-199

Filter Cake Formation on Deep Vertical Well Under High Pressure and Temperature Conditions Computational Fluid Dynamics Modeling and Simulations

Ahmed M.Ramadan [a*], Mohamed F.Shehadeh[a], Ali I. Shehata[a], Ahmed Mehanna[a].

[a] *College of Engineering and Technology, Arab Academy for Science, Technology and Maritime Transport, P.O. Box 1029, Abu Qir, Alexandria, Egypt.*

**Corresponding authors*

Abstract

The study of drilling fluid behavior is critical for a successful drilling operation. Drilling fluids are slurries consists of solid particles suspended in a liquid phase. Due to the differential pressure, the liquid phase of the drilling mud invades into a permeable formation leaves solid particles on the formation walls forming a filter cake. A basic drilling fluid should be designed, to seal permeable zones as quickly as possible with thin, slick filter cakes and fluid loss control. Thick filter cakes and excessive filtration lead to tight hole, increased torque and drag, stuck pipe, lost circulation, poor log quality, and formation damage. Control fluid invasion to form a thin, low-permeability filter cake are often necessary to prevent drilling and production problems. The focus of this research is to use a 3D-computational fluid dynamics (CFD) technique to numerically simulate filter cake formation with pipe rotation on a vertical wellbore wall at deep drilling conditions (high-pressure (25,500 psi or 175.8 MPa) and temperature (170°C)) and at shallow drilling conditions (pressure (2,000 psi or 13.8 MPa) and temperature (30° C)). Here, the drilling fluids treated as a two-phase system in which solid particles suspended in non-Newtonian fluid using an Eulerian-Eulerian approach. Drilling simulations performed for drilling fluid with pipe rotation and particle size 50 μm, under high pressure and temperature drilling conditions and successfully predicted a filter cake thickness, which agrees well with measurements and literature of CFD analysis in this area. The results comparison clearly shows that filter cake formed for both scenarios on the vertical wellbore wall is non-uniform and the filter cake thickness formed for deep drilling operation is thicker than that formed for shallow drilling operation.

Key words: Filter cake, two-phase flow, computational fluid dynamics (CFD), deep drilling.

1. INTRODUCTION

Drilling fluids are slurries composed of a liquid phase and solid particles. One of the major factors that affect the process performance is the adjusting of drilling fluid composition and type.

Because of the Drilling operation, one of the critical operations in the oil and gas field that involve several issues require robust and efficient guidelines. During the drilling process, multiphase drilling fluids pumped down through the drilling string and circulated continuously to perform several tasks, such as: Remove cuttings from the well, Control formation pressures, Suspend and release cuttings, Seal permeable formations, Maintain wellbore stability, Minimize reservoir damage, Cool, lubricate, and support the bit and drilling assembly, Transmit hydraulic energy to tools and bit, Ensure adequate formation evaluation, Control corrosion, Facilitate cementing and completion and Minimize impact on the environment. The liquid phase of the drilling mud forced into a permeable formation by differential pressure between the hydrostatic pressure of the mud column and the formation pressure referred to as the filtration process, the solid particles filtered out forming the filter cake. This filter cake is essential to preserve the borehole and protect it from collapsing [1-4]. Many factors can affect the filter cake formation process such as drill string RPM, annulus velocity, drilling fluid type, solid particle size, formation temperature, formation pressure, and formation permeability [5-8]. The presentation of the earliest researches and studies applied on mud filtration directed at formulating additives to provide properties matching the API (American petroleum institute) test and results standards. Ershaghi et al., 1980 [9] developed a numerical simulation techniques to minimize the laboratory data requirement in filtration mathematical models. The study confirmed the effect of filtrate viscosity and cake permeability on filtrate volumes. Tien and R. Bai, 2003 [10] proposed an iterative procedure of predicting filtration performance; procedures are based on the assumption that the pressure drop across the filter cake is the same as the operating pressure. This assumption is often justified on the basis that the average specific cake resistance is high and therefore, the pressure drop across the medium can ignored. Moreover, observed that the conventional filtration theory under-predicts parameters and suggested improvements based on better estimation of the average specific cake resistance and the wet cake to dry cake mass ratios. Tan et al., 2008 [11] proposed the equivalent cake filtration modeling to describe filtration in Newtonian and non-Newtonian fluids. Focuses on predicting filtration quality and calculating cake specific resistance based on operational parameters. In addition, evaluated an equation could be used as a prediction of filtrate

rate for both Newtonian and non-Newtonian fluids. Kabir and Gamwo, 2011 [6] numerically simulated filter cake formation process at the bottom of a laboratory-scale pressure filtration cell. Filter cake formation data extracted from single pressure filtration CFD simulations and compared with analytically calculated filter cake height to verify the agreement of the numerical simulation validity. Elkatatny, Mahmoud, Nasr-El-Din, et al., 2012 [12] Investigated experimentally that the filter cake was thinner and had a lower permeability under dynamic conditions than was the case under static conditions. The results obtained from the computed tomography (CT) scan, showed that the filter cake was heterogeneous with a different properties under various conditions, a new method developed to measure the thickness of the filter cake, and various model screened to identify the best model that can predict specific permeability measurements.

Drilling process and filter cake formation

Drilling fluids are slurries consists of solid particles suspended in a liquid phase, this multiphase fluid pumped down through the drill pipe and interacts with formation cuttings. The overbalance between the drilling fluid hydrostatic pressure and formation pressure cause a differential pressure which force the combination of drilling fluid and formation cuttings into the porous rock formation and build the filter cake. The fluid invade porous rock formation called filtrate leaves solid particles on the porous rock surface in the form of filter cake. The quantity of fluid invasion that invades in the porous rock formation depend on several factors like rock formation resistance, formation porosity, formation permeability, fluid density, solid particle size, solid particle distribution, fluid viscosity, and differential pressure, this relationships described by Darcy's Law [13-16]. The filter cake thickness depends on the concentration of mass loading per unit area (kg/m2) and specific resistance (m/kg) which resist and decrease fluid invasion into porous rock formations [13, 16].

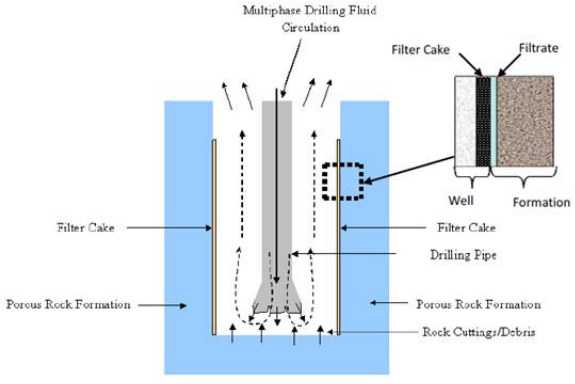

Fig.1: illustrates filtration mechanism

Literature review further reveals that no filter cake formation modeling has yet been performed for deep deviated drilling conditions under high temperature and high pressure. Most of the previous research carried out with Newtonian, single-phase, and isothermal conditions for the shallow drilling process. The objectives of the present study were to establish a 3D model of filter cake formation for deep drilling conditions at high temperature and high pressure by using CFD OpenFoam software, This simulation is capable of predicting the filtration process with conditions similar to deep wellbore drilling, validate such model, and investigate its sensitivity to boundary conditions.

2. MULTIPHASE FLOW AND GOVERNING EQUATIONS

The CFD modeling and simulations involved the solution of Naiver-Stokes equations. Hence, detailed equations of multiphase fluids and their relevant theories also provided here. The dynamics of solids-in-fluid media have a large effect on various flow phenomena, such as density, viscosity, and pressure. Thus, the hydrodynamics of solids must modeled correctly [17]. The Eulerian approach is preferred over the Lagrangian due to the large volume fraction of solids in the drilling fluid. In the Eulerian approach, fluid and solid phases treated as interpenetrating continua, and momentum and continuity equations are defined for each phase [18]. Therefore, the Eulerian-Eulerian multiphase fluid model used to simulate fluid flow and filter cake formation in vertical wellbore drilling operations for shallow and deep drilling conditions. The Eulerian model is the most complex of the multiphase models, solving a set of n momentum and continuity equations for each phase. Coupling achieved through the pressure and inter-phase exchange coefficients. The manner in which this coupling handled depends upon the type of phases involved. For granular flows, properties obtained by applying kinetic theory. Mass transfer between the phases is negligible and, therefore, ignored here. The momentum equation for the solid phase differs from the equation used for the fluid phase, since the former contains a solid pressure [18-20]. Lift and virtual mass forces assumed negligible in the momentum equations.

2.1 Mathematical model

The CFD model presented herein adopted steady, incompressible, laminar two-phase flow assumptions, with non-Newtonian power law viscosity. The model details can found in OpenFoam theory guide. Therefore, neglecting the intra-phase mass transfer and any external sources, the conservation of mass in the model can expressed as:

Conservation of mass

For liquid, $\nabla.(\alpha_l \ \nu_l) = 0$ (1)

For solids, $\nabla.(\alpha_s \ \nu_s) = 0$ (2)

Where α is the volume fraction and subscripts l and s denote liquid and solid phases, respectively. Moreover, $\alpha_l + \alpha_s = 1$ must be satisfied. In addition vl, vs are the velocities of the solid and liquid phases.

The momentum equation for the liquid phase in a solid-liquid system expressed as:

$$\nabla.(\alpha_l \rho_l \overrightarrow{v_l}\,\overrightarrow{v_s}) = \underbrace{-\alpha_l \nabla P + \nabla.\overline{\tau_1}}_{\text{Convective pressure}} + \underbrace{\alpha_l \rho_l \vec{g}}_{\text{Stress body forces}} - \underbrace{\{K_{sl}\,(\overrightarrow{v_l} - \overrightarrow{v_s})\}}_{\text{Momentum exchange}} \quad (3)$$

Where ρ_l and ρ_s are the densities of liquid and solid phases, ∇P is the pressure gradient $\overline{\tau_1}$ is the stress tensor of the liquid phase, which is related to the strain

$\overline{\dot{\gamma}_l} = \nabla\overrightarrow{v_l} + (\nabla\overrightarrow{v_l})^{tr}$ By $\overline{\tau_1} = \alpha_l \tau\ \overline{\dot{\gamma}_l} + \alpha_l \left(\lambda_l - \frac{2}{3}\tau\right)\nabla.\overrightarrow{v_l}\,\bar{\mathrm{I}}$

Where tr is transitional velocity, $\tau = k\left|\overline{\dot{\gamma}_l}\right|^{n-1}$ and $\left|\overline{\dot{\gamma}_l}\right|$ is the magnitude of the strain rate tensor defined-as: $\left|\overline{\dot{\gamma}}\right| = \sqrt{\frac{1}{2}\sum_i \sum_j \dot{\gamma}_{ij}\,\dot{\gamma}_{ji}}$

and, k and n are consistency factor and power-law exponent, respectively

The momentum equation for the solid phase in a solid-liquid system can expressed as:

$$\nabla.(\alpha_s \rho_s \overrightarrow{v_s}\overrightarrow{v_s}) = -\alpha_s \nabla P - \nabla P_s + \nabla.\overline{\tau_s} + \alpha_s \rho_s \vec{g} + \{(K_{ls}(\overrightarrow{v_l} - \overrightarrow{v_s}))\} \quad (4)$$

The solids pressure,P_s stress, $\overline{\tau_s}$ and viscosity, μ_s determined by particle fluctuations and the kinetic energy associated to these fluctuations, granular temperature Θ. The stress-strain relationship for the solid phase s is $\overline{\tau_s} = \alpha_s \mu_s \overline{\dot{\gamma}_s} + \alpha_s \left(\lambda_s - \frac{2}{3}\mu_s\right)\nabla.\overrightarrow{v_s}\,\bar{\mathrm{I}}$ Where solid strain rate tensor. $\overline{\dot{\gamma}_s} = \nabla\overrightarrow{v_s} + (\nabla\overrightarrow{v_s})^{\mathrm{tr}}$

Interaction forces considered here to account for the effects of other phases and reduced to zero for single-phase flow.

The momentum exchanges coefficients are in distinguish-able ($K_{ls} = K_{\mathrm{sl}}$), $K_{\mathrm{sl}} = \frac{\alpha_s \rho_s f}{\mathrm{T}_s^p}$ This function and coefficients are suitable for drilling process modeling where recirculation multiphase fluids contain high solid fraction.

T_s^p Here, is the particulate relaxation time and is the model-dependent drag function. The relaxation time is expressed as $\mathrm{T}_s^p = \frac{\rho_s {d_s}^2}{18\mu_l}$ where d_s is the solid particle diameter.

The Syamlal-O'Brien drag function used$f = \frac{C_D Re_s \alpha_l}{24\,{v^2}_{r,s}}$ to describe the conservation of energy in Eulerian multiphase applications, a separate steady-state enthalpy equation can written for each phase q (liquid or solid) as follows:

$\nabla.\left[\alpha_q \rho_q \overline{u_q} h_q\right] = \overline{\tau_q}:\nabla\overline{u_q} - \nabla.\overline{q_q} + \sum_{p-1}^{n}\left[\overline{Q_{pq}}\right]$ (5) Where h_q is specific phase enthalpy, $\overline{q_q}$ is the heat flux, and $\overline{Q_{pq}}$ is the intensity of heat exchange between phases [17,21].The multiphase fluid flow through the porous rock is modeled using an extension of Darcy's law for multiphase flow, also referred to as the Ergun equation for laminar flow or the Blake-Kozeny equation. This equation reads: $\nabla P = -\frac{\mu}{K_p} v$ (6) where v is the seepage fluid velocity in the formation and μ the fluid dynamic viscosity. The porous media permeability, Kp, is given below in terms of formation porosity (ε) and the porous media mean pore size (DP). Here, we set a formation void fraction of 0.2 following [15]: $K_p = \frac{{D_p}^2}{150}\frac{\varepsilon^3}{(1-\varepsilon)^2}$ (7) the differential pressure in between the porous media formation and annulus maintained at 500 psi (3.4 MPa).

3. COMPUTATIONAL MODEL VALIDATION

3.1. Model description

The computational domain decomposed of 6000 Hexahedral cells (30 x 200x 1) with Dirichlet boundary conditions for the pressure field at the inlet and outlet plans of the domain.

Absolute residuals of the iterative solver used as a criteria convergence and were set to a value of 1×10-4 for both velocity and pressure. Convective term discretized with Central difference discretization scheme used, and the SIMPLE algorithm used to couple the velocity and pressure terms in the governing equations. The simulation performed for pressure filtration where inlet pressure kept at 100 kPa. The filtration cell initially filled with multiphase particulate drilling fluid, and the pressure applied at the top (inlet) with porous media at the bottom (outlet).

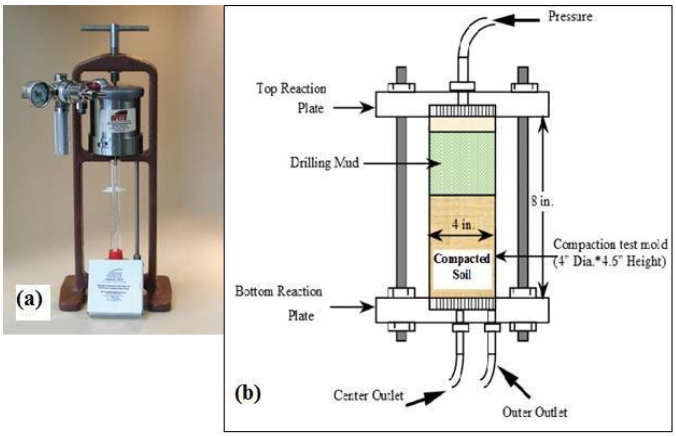

Fig. 2: API filter press

The literature review shows a little data available on experimental and numerical results to validate the application

of CFD in simulation for filter cake formation [22]. A transient CFD simulation of a single linear pressure filtration cell was set up.

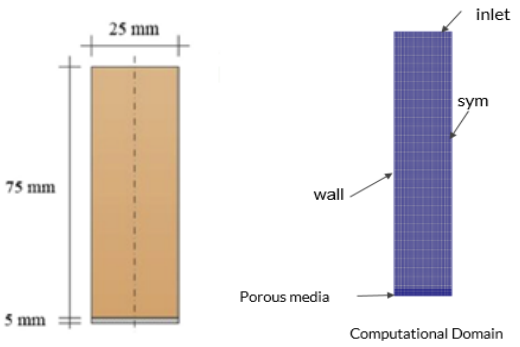

Fig.3: shows the geometry of the filtration cell &**Fig. 4:** shows the half domain generated mesh.

3.2. Initial and boundary conditions

A two-dimensional (2-D) model created assumed symmetry along the central axis; simulate half domain to reduce the run time with same accuracy. The entire domain consists of multiphase drilling fluid and the porous media. The multiphase drilling fluid composed of a liquid phase and solid particles with 0.185 volume fraction for the solid particles and 0.815 for water phase. Based on the value of porosity and the mean solid particle diameter calculated using the equation (7). The porous media permeability was considered 135 mD. The Power Law model used for modeling the fluid behavior. The water phase was set as the primary phase and the solid phase was set as the secondary phase in the granular Eulerian model, The Eulerian model used to simulate the multiphase drilling fluid flow because the concentration of secondary phase (solid phase) in the multiphase flow is more than 10%. The solid phase defined as a continuous phase with granular behavior and the drag interaction between the primary phase (water) and secondary phase (solid) defined by modified Syamlal-Obrien model. The Syamlal-Obrien model and Lun et al. model used for modeling the viscosity and the granular bulk viscosity in solid phase [23]. K-ε turbulence model used to simulate the fluid flow zone and the porous zone was set to have a laminar [24]. Based on the filter cake experimental operating conditions, the inlet boundary condition was set at 100 kPa as the total gauge pressure. Stationary wall was set at the left end of the model while the right side was set as the symmetry boundary condition. The outlet at the bottom of computational mesh as the outlet-vent boundary condition.

Table 1: shows the parameters for current model and past models

Parameters	Kabir Model	Current Model
Thickness (mm)	2.5 mm	5 mm
Permeability of porous (mD)	135	135
Density of drilling fluid (Kg/m3)	1248	1248
Solid fraction	0.185	0.185
Mean diameter of particles (microns)	50	50

3.3 Validation

At the beginning, the water phase only start to inflowing the domain from the top inlet and applied 100-kPa pressure on the multiphase fluid. The multiphase fluid (solid and water mixture) passing through the porous zone, the filter cake layer starts to build up and accumulate as both filter cake thickness and solid volume fraction increase with the time. During simulation, the maximum solid phase volume fractions remains almost constant while the filter cake thickness only increases as shown in figure 5. Figure 6 shows the profile of solids volume fraction at the end of simulation conducted by Kabir and in current model, which shows a good agreement between the results [6].

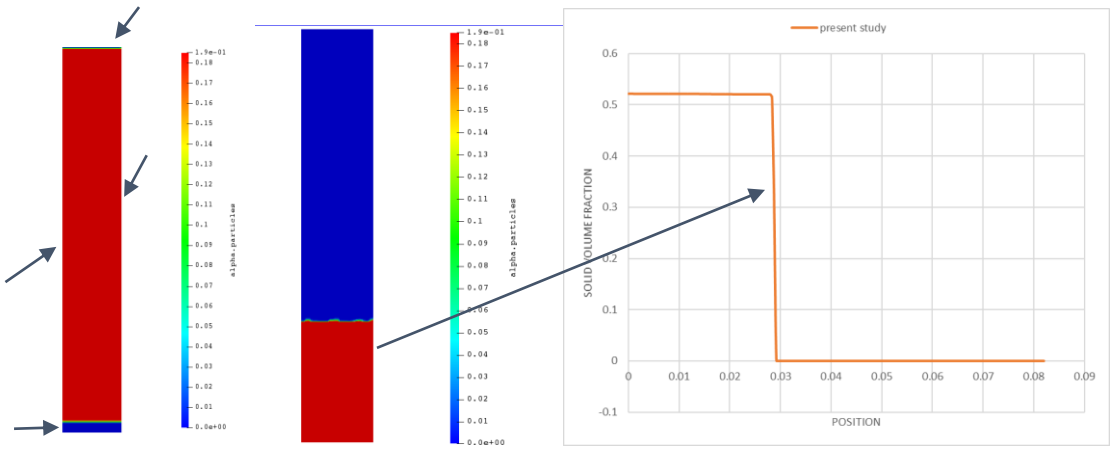

Fig. 5: shows the contours of solid volume fraction at the beginning and at the end of the simulation.

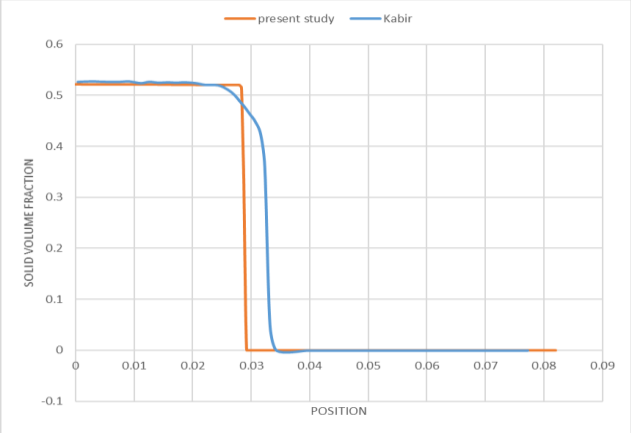

Fig. 6: shows the profile of solids volume fraction at the end of simulation conducted by Kabir and in current model [6].

A CFD model for the filter cake formation process in well-bore drilling was constructed using two-phase Eulerian solver in OpenFOAM (twoPhaseEularFoam). The model employed an Eulerian-Eulerian multi-phase formulation and a non-Newtonian power-law viscosity model. The model results validated against previous CFD work, experimental measurements and analytical predictions of filter cake thickness. As shown in figure 7 the model results showed a good agreement with previous works, which proved the model validity and reliability for mimicking well-bore filter cake formation processes.

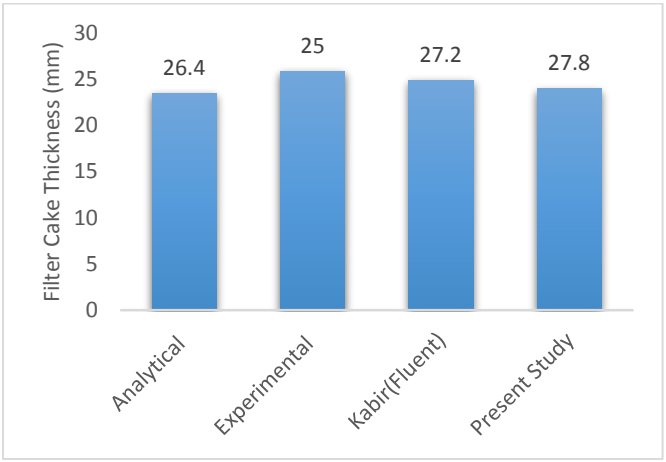

Fig. 7: shows that the present CFD model is in good agreement with analytical model as well as the experimental model.

4. MODELING FOR VERTICAL WELL

4.1Three-dimensional vertical wellbore model

A three-dimensional (3-D) well bore model of a vertical well was constructed and meshed with ICEM CFD as shown in Figure 9,10 To simulate the drilling process, multi-phase particulate (αs = 0.2) drilling fluid was pumped into the model inlet, and multi-phase particulate (αs = 0.8) rock debris was pushed from the bottom inlet. The model inlet represents drilling fluid pumping in, and the bottom inlet represents rock debris that accumulates during drilling. The solid wall represents the drill string surface. A porous medium with next to the drill string represents the vertical rock formations on which filter cake builds up. The pressure and temperature are 25,500 psi (175.8 MPa) and 170 °C, respectively, for deep drilling conditions. The formation pressure and temperature maintained at 25,000 psi (172.4 MPa) and 170 °C to mimic real-world drilling scenarios as shown in Figure 6. Multi-phase particulate non-Newtonian drilling fluids pumped into the drilling zone where the drilling fluids mixed with rock particles. The particle-laden drilling fluid then flowed upwardly, back to the surface, through the annulus between the walls or sides of the well bore and the drill string as shown in figure 8.

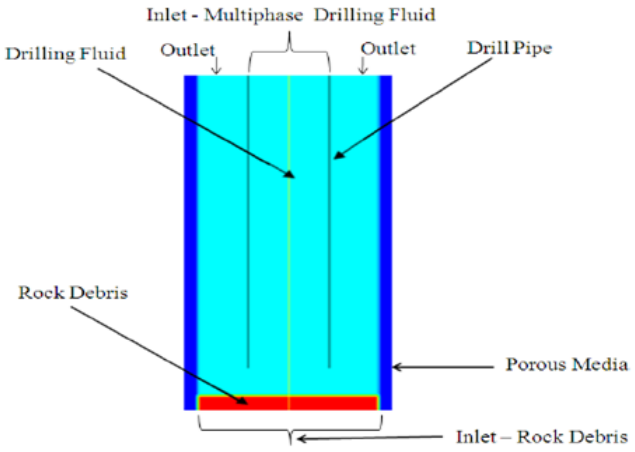

Fig. 8: Initial solid volume fraction distribution in the well

4.1.1 Initial and boundary conditions

As mentioned earlier, axis-symmetry assumed for modeling the drilling process. The domain discretized with grid where the flow domain divided into finite surfaces. As mentioned earlier, a fully rotating 3-D transient consideration for the modeling the drilling process. Several trials were made (from 40,000 to 120,000 meshes) to verify grid independent results from CFD simulations.

A multiphase (solid/liquid) drilling fluid pumped from the upper inlet and the bottom filled with rock debris represent formation cuttings. The density of the liquid phase was 999 kg/m3 with consistency (k) 0.1238 Pa.sn and power-law (n) index of 0.67 the liquid phase is under non-Newtonian power-law fluid properties. The solid phase density was set at 2,350 kg/m3 under granular properties with 50-μm particle size [16, 25]. A Three-dimensional CFD simulation performed to simulate filter cake formation thickness and distribution along 1 meter long in radial direction on vertical well walls during deep and shallow drilling operations. Both initial and boundary conditions are close similar to field operation conditions as per table [14-15, 25-33].

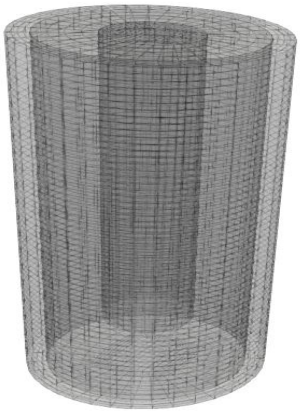

Fig.9: (3-D) Computational Domain

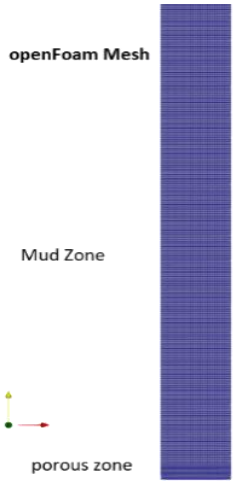

Fig. 10: Grid Mesh

Table 2: shows the parameters for shallow and deep well

Parameters	Shallow Well	Deep Well
Inlet pressure (drilling fluid/top), Psi or MPa	2,000 or 13.8	25,500 or 175.8
Pressure (bottom), Psi or MPa	2,000 or 13.8	25,500 or 175.8
Outlet pressure, Psi or MPa	1,500 or 10.3	25,000 or 172.4
Formation pressure (porous media), Psi or MPa	1,500 or 10.3	25,000 or 172.4
Particle size, micron	50	50
Formation porosity	0.2	0.2
Temperature, C	30	170
Solid fraction (drilling fluid/top)	0.2	0.2
Solid fraction (rock/bottom)	0.8	0.8
Particle density, Kg/m3	2350	2350
Fluid density, Kg/m3	999	999

4.2 Results and discussion

4.2.1 Comparison of deep and shallow drilling simulations

Our (3-D) model with pipe rotation shows a good agreement with Kabir (2-D) model for both scenario shallow and deep drilling as shown in figure 11, 12 and 13. The filter cake thicknesses extracted from the solid fraction graph for both shallow and deep drilling conditions with the same particle size 50 μm as figures presented. Observed also that the filter cake for both deep and shallow condition was non-uniform distribution as the filter cake thickness is thinner in the lower bottom portion of the well followed by a thicker cake at the upper portion of the well. Figure 13 compares the simulated filter cake thickness for both deep and shallow drilling conditions. It clearly shows thicker cake for deep drilling conditions. The average cake thickness is 0.05 m for deep drilling processes and 0.0140 m for shallow drilling. Hence, the higher pressure and temperature environment favors thicker cake formation. The non-uniformity of the filter cake thickness in both shallow and deep drilling conditions depends on the value and the magnitude of the vortices in the annulus between the wellbore walls and drill string in which affects the filter cake thickness. As the large vortices value form, a thin filter cake thickness in the bottom portion compared to smaller vortices value form a thicker filter cake at the top portion.

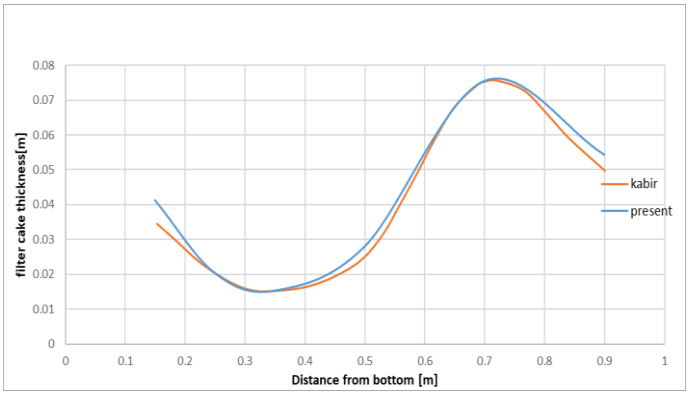

Fig. 11: comparison of cake thickness distribution along deep well (Kabir vs present study)

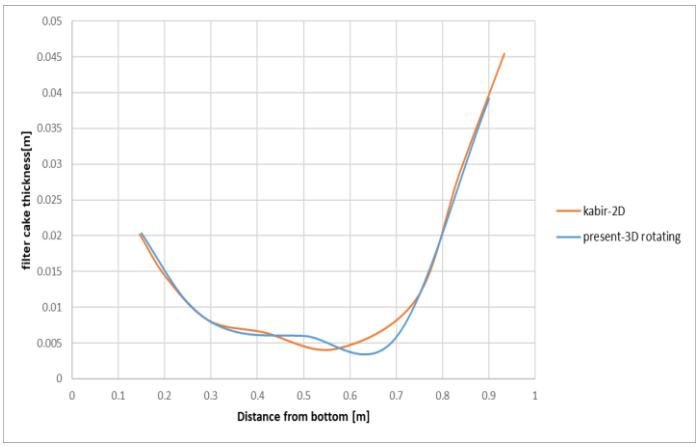

Fig. 12: comparison of cake thickness distribution along shallow well (Kabir vs present study)

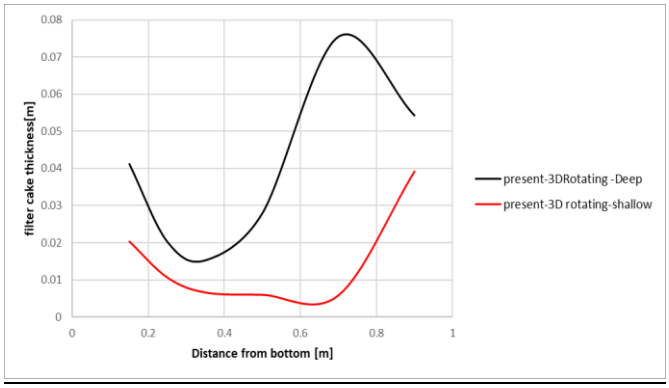

Fig. 13: compares the simulated filter cake thickness for both deep and shallow drilling conditions.

5. CONCLUSION

Control Fluid invasion and filter cake thickness has significant effect on cake properties, penetration rate and formation damage which interfere various drilling and completion operations. This research study shows a good agreement with both experimental and analytical studies, this paper used computational fluid dynamic simulations to validate and simulate the filtration mechanism for vertical deep drilling under high pressure and temperature conditions.

The interlinked solution aspects had solved with three-dimensional (3-D) wellbore vertical model for multiphase non-Newtonian fluid flow in the pipe and in the annulus between the drill pipe and the borehole taking the aspect of drill pipe rotation into consideration and the effects of drilling fluid particle sizes on the filter cake thickness also studied. The results shows filter cake thickness and solid volume fractions are higher for deep drilling operation compared to shallow drilling this is because the high pressure and high temperature conditions, also the vortices from the drill pipe rotation clearly lead to non-uniform filter cake distribution on the well wall.

REFERENCES

[1] Argillier, J.F., Audibert, A., Bailey, L. and Reid, P.I., IFP Energies Nouvelles IFPEN and Dowell Schlumberger Inc, 1997. *Process and water-base fluid for controlling the dispersion of solids application to drilling*. U.S. Patent 5,637,556.

[2] Benna, M., Kbir-Ariguib, N., Clinard, C. and Bergaya, F., 2001. Static filtration of purified sodium bentonite clay suspensions. Effect of clay content. *Applied Clay Science*, *19*(1-6), pp.103-120.

[3] Khodja, M., Canselier, J.P., Bergaya, F., Fourar, K., Khodja, M., Cohaut, N. and Benmounah, A., 2010. Shale problems and water-based drilling fluid optimisation in the Hassi Messaoud Algerian oil field. *Applied Clay Science*, *49*(4), pp.383-393.

[4] Blkoor, S.O. and Fattah, K.A., 2013. The influence of XC-polymer on drilling fluid filter cake properties and formation damage. *J. Pet. Environ. Biotechnol*, *4*(5).

[5] Chenevert, M.E. and Dewan, J.T., 2001. A model for filtration of water-base mud during drilling: determination of mudcake parameters. *Petrophysics*, *42*(03).

[6] Kabir, M.A. and Gamwo, I.K., 2011. Filter cake formation on the vertical well at high temperature and high pressure: computational fluid dynamics modeling and simulations. *Journal of Petroleum and Gas Engineering*, *7*(2), pp.146-164.

[7] Ozyurtkan, M.H., Altun, G., Ettehadi Osgouei, A. and Aydilsiz, E., 2012, January. Dynamic filtration properties of clay based drilling muds under elevated temperatures. In *SPE Kuwait International Petroleum Conference and Exhibition*. Society of Petroleum Engineers.

[8] Li, X., Jaffal, H., Feng, Y., El Mohtar, C. and Gray, K.E., 2018. Wellbore breakouts: Mohr-Coulomb plastic rock deformation, fluid seepage, and time-dependent mudcake buildup. *Journal of Natural Gas Science and Engineering*, *52*, pp.515-528.

[9] Ershaghi, I., 1980, January. Modeling of Filter Cake Buildup Under Dynamic-Static Conditions. In *SPE California Regional Meeting*. Society of Petroleum Engineers.

[10] Tien, C. and Bai, R., 2003. An assessment of the conventional cake filtration theory. *Chemical Engineering Science*, *58*(7), pp.1323-1336.

[11] Tan, X.U., Qixin, Z.H.U., Xu, C.H.E.N. and Wenping, L.I., 2008. Equivalent cake filtration model. *Chinese Journal of Chemical Engineering*, *16*(2), pp.214-217.

[12] Elkatatny, S., Mahmoud, M.A. and Nasr-El-Din, H.A., 2012. Characterization of filter cake generated by water-based drilling fluids using CT scan. *SPE Drilling & completion*, *27*(02), pp.282-293.

[13] Fu, L.F. and Dempsey, B.A., 1998. Modeling the effect of particle size and charge on the structure of the filter cake in ultrafiltration. *Journal of membrane Science*, *149*(2), pp.221-240.

[14] Cerasi, P. and Soga, K., 2001. Failure modes of drilling fluid filter cake. *Geotechnique*, *51*(9), pp.777-785.

[15] Parn-Anurak, S. and Engler, T.W., 2005. Modeling of fluid filtration and near-wellbore damage along a horizontal well. *Journal of Petroleum Science and Engineering*, *46*(3), pp.149-160.

[16] Fisher, K.A., Wakeman, R.J., Chiu, T.W. and Meuric, O.F.J., 2000. Numerical modelling of cake formation and fluid loss from non-Newtonian muds during drilling using eccentric/concentric drill strings with/without rotation. *Chemical Engineering Research and Design*, *78*(5), pp.707-714.

[17] Cornelissen, J.T., Taghipour, F., Escudié, R., Ellis, N. and Grace, J.R., 2007. CFD modelling of a liquid–solid fluidized bed. *Chemical Engineering Science*, *62*(22), pp.6334-6348.

[18] Medina, H., Beechook, A., Saul, J., Porter, S., Aleksandrova, S. and Benjamin, S., 2015. Open source computational fluid dynamics using OpenFOAM. In *Royal Aeronautical Society, General Aviation Conference, London*.

[19] Ishii, M., 1975. Thermo-fluid dynamic theory of two-phase flow. *NASA Sti/recon Technical Report A*, *75*, p.29657.

[20] Jackson, R., 1997. Locally averaged equations of motion for a mixture of identical spherical particles and a Newtonian fluid. *Chemical Engineering Science*, *52*(15), pp.2457-2469.

[21] Fordham, E.J., Ladva, H.K.J., Hall, C., Baret, J.F. and Sherwood, J.D., 1988, January. Dynamic filtration of bentonite muds under different flow conditions. In *SPE Annual Technical Conference and Exhibition*. Society of Petroleum Engineers.

[22] Saha, H., 2009. Pratical application of filtration theorey to the minerals industry. *The University of Melbourne, Australia, PhD Thesis*.

[23] Syamlal, M., Rogers, W. and OBrien, T.J., 1993. *MFIX documentation theory guide* (No. DOE/METC-94/1004). USDOE Morgantown Energy Technology Center, WV (United States).

[24] Launder, B.E. and Spalding, D.B., 1983. The numerical computation of turbulent flows. In *Numerical prediction of flow, heat transfer, turbulence and combustion* (pp. 96-116). Pergamon.

[25] Hamed, S.B. and Belhadri, M., 2009. Rheological properties of biopolymers drilling fluids. *Journal of Petroleum Science and Engineering*, *67*(3-4), pp.84-90.

[26] Vaussard, A., Martin, M., Konirsch, O. and Patroni, J.M., 1986, January. An experimental study of drilling fluids dynamic filtration. In *SPE Annual Technical Conference and Exhibition*. Society of Petroleum Engineers.

[27] Delhommer, H. J., & Walker, C. O. (1987). Method for controlling lost circulation of drilling fluids with hydrocarbon absorbent polymer. US Patent Number, 4:633,950.

[28] Sherwood, J.D., Meeten, G.H., Farrow, C.A. and Alderman, N.J., 1991. Concentration profile within non-uniform mudcakes. *Journal of the Chemical Society, Faraday Transactions*, *87*(4), pp.611-618.

[29] Rogers, H.E., Murray, D.A. and Webb, E.D., Halliburton Co, 1996. *Apparatus and method for removing gelled drilling fluid and filter cake from the side of a well bore*. U.S. Patent 5,564,500.

[30] Usher, S.P., De Kretser, R.G. and Scales, P.J., 2001. Validation of a new filtration technique for dewaterability characterization. *AIChE Journal*, *47*(7), pp.1561-1570.

[31] Spooner, K.M., Bilbo, D. and McNeil, B., 2004, April. The application of high temperature polymer drilling fluid on Smackover operations in Mississippi. In *AADE-2004 Drilling Fluids Conference. Houston, Texas*.

[32] Ali, S., Bowman, M., Luyster, M.R., Patel, A., Svoboda, C., McCarty, R.A. and Pearl, B., 2004. Reversible drilling-fluid emulsions for improved well performance. *Oilfield Review*, *16*(3), pp.62-68.

[33] Berry, J.H., 2009. Drilling fluid properties & function, CETCO drilling products.